Journal of Organometallic Chemistry 897 (2019) 32–41

Contents lists available at ScienceDirect

Journal of Organometallic Chemistry

journal homepage: www.elsevier.com/locate/jorganchem

Triphenylantimony(V) catecholato complexes with 4-(2,6-dimethylphenyliminomethyl)pyridine. Structure, redox properties: The influence of pyridine ligand

Ludmila S. Okhlopkova [a], Andrey I. Poddel'sky [a, *], Ivan V. Smolyaninov [b], Georgy K. Fukin [a], Nadezhda T. Berberova [c], Vladimir K. Cherkasov [a], Gleb A. Abakumov [a]

[a] G.A. Razuvaev Institute of Organometallic Chemistry of Russian Academy of Sciences, 603137, Nizhniy Novgorod, 49 Tropinina Str, Russia
[b] Southern Scientific Centre of Russian Academy of Sciences, 344006, Rostov-on-Don, 41 Chekhova Str, Russia
[c] Astrakhan State Technical University, 414025, 16 Tatisheva Str, Russia

ARTICLE INFO

Article history:
Received 10 June 2019
Accepted 19 June 2019
Available online 21 June 2019

Keywords:
Redox-active ligand
Catecholate
Iminopyridine
Antimony(V)
X-ray analysis
Cyclic voltammetry

ABSTRACT

The complexation of triphenylantimony(V) catecholates (3,6-DBCat)$SbPh_3$ (**1**), (4,5-pip-3,6-DBCat)$SbPh_3$ (**2**) and (4,5-Cl_2-3,6-DBCat)$SbPh_3$ (**3**) with neutral 4-(2,6-dimethylphenyliminomethyl)pyridine (Py-CH=N–Ar) leads to the formation of hexacoordinated complexes (3,6-DBCat)$SbPh_3$·(Py-CH=N–Ar) (**4**), (4,5-pip-3,6-DBCat)$SbPh_3$·(Py-CH=N–Ar) (**5**) and (4,5-Cl_2-3,6-DBCat)$SbPh_3$·(Py-CH=N–Ar) (**6**) (where 3,6-DBCat is 3,6-di-*tert*-butyl-catecholate, 4,5-pip-3,6-DBCat is 4,5-(*N*,*N*′-piperazine-1,4-diyl)-3,6-di-*tert*-butyl-catecholate, 4,5-Cl_2-3,6-DBCat is 4,5-dichloro-3,6-di-*tert*-butyl-catecholate) containing $N_{Pyridine}$-coordinated neutral donor ligand Py-CH=N–Ar. In the absence of donor ligands chlorine-containing catecholate **3** undergoes rearrangement in acetonitrile to form ionic complex $[Ph_4Sb]^+[(4,5\text{-}Cl_2\text{-}3,6\text{-}DBCat)_2SbPh_2]^-$ (**7**). Complexes have been isolated and characterized by spectroscopic methods and cyclic voltammetry. The pyridine-containing catecholate (3,6-DBCat)$SbPh_3$·Py (**8**) was also synthesized in order to compare it's the electrochemical behaviour with those of iminopyridine complexes **4**–**6**. The presence of $N_{Pyridine}$-coordinated iminopyridine ligand changes the mechanism of catecholate oxidation in **4** and **6**: the first oxidation wave (at $E^{ox1}_p = 0.94$ V for **4** and 0.99 V for **6**) is two-electron and corresponds to the oxidation of dianionic catecholate ligand to a coordinated *o*-benzoquinone. In contrast to catecholates **4** and **6**, the electrochemical behaviour of piperazine-containing catecholate **5** does not practically differ from that one for initial catecholate **2**. The molecular structures of complexes **3**–**7** in crystals have been determined by single-crystal X-ray analysis.

1. Introduction

The antimony compounds find an application as the components of polymerization catalysts, reagents in fine chemical synthesis, antiseptic agents, antioxidants and much more [1]. The variety of structural types, coordination possibilities, Lewis acidity properties of antimony-containing complexes [2] makes them to be attractive objects for the development of fundamental ideas about the "structure-property" influences in the coordination chemistry. In the case of antimony(V) catecholates, in the absence of steric hindrances, the metal center is able to complete its coordination number to six [3] by means of the intermolecular interactions or the additional neutral donor ligands. The introduction of the donor ligands to the metals coordination sphere has a significant impact on the structure, magnetic properties [4], redox properties of the complexes formed [5]. Iminopyridines represent a widely used class of neutral ligands [6]. However, iminopyridines can also serve as the redox-active ligands forming radical-anionic and dianionic derivatives [7]. Their metal complexes possess the wide variability of the molecular and electronic structure, and such compounds are the attractive and interesting objects for both the fundamental and applied sciences (a design of catalysts, coordination polymers, MOFs, polyfunctional materials etc) [8,9]. A combination of antimony(V) complexes containing redox-active catecholate ligand with iminopyridine as *N*-donor ligand should cause modifications in the chemical and electrochemical behaviour of such complexes which is of interest in the

* Corresponding author.
E-mail address: aip@iomc.ras.ru (A.I. Poddel'sky).

https://doi.org/10.1016/j.jorganchem.2019.06.025
0022-328X/

view of their potential application as radical scavengers [10], O_2-binding agents and carriers [11], destructors of peroxides [12] etc. In the present paper we report on the complexation of mononuclear triphenylantimony(V) 3,6-di-*tert*-butyl-catecholate (3,6-DBCat) and related complexes containing electron donor- (piperazine-1,4-diyl) or acceptor (chlorine) substituents in 4th and 5th positions of 3,6-DBCat ligand with the additional neutral *N*-donor ligand 4-(2,6-dimethylphenyliminomethyl)pyridine (Py-CH=N–Ar).

2. Experimental

2.1. General considerations

Solvents were purified by standard methods [13]. Syntheses of complexes were carried out in vacuum. The ^{1}H and ^{13}C NMR spectra were recorded on Bruker AVANCE DPX-200 spectrometer, using the $CDCl_3$ solvent and the internal standard tetramethylsilane. The IR spectra were recorded on Specord M-80. The X-ray structure analysis was carried out on "Smart Apex" diffractometer (Bruker AXS).

4,5-(*N,N′*-piperazine-1,4-diyl)-3,6-di-*tert*-butyl-*o*-benzoquinone, 4,5-di-chloro-3,6-di-*tert*-butyl-*o*-benzoquinone, (3,6-di-*tert*-butyl)-catecholato)triphenylantimony(V) (3,6-DBCat)$SbPh_3$ (**1**), 4,5-(*N,N′*-piperazine-1,4-diyl)-3,6-di-*tert*-butyl-catecholato)triphenylantimony(V) (4,5-pip-3,6-DBCat)$SbPh_3$ (**2**) were synthesized by the known methods [14–16], 4-(2,6-dimethylphenyliminomethyl)pyridine - as described in Ref. [17].

2.2. Synthesis

2.2.1. (4,5-Dichloro-3,6-di-tert-butyl-catecholato) triphenylantimony(V) (4,5-Cl_2-3,6-DBCat)$SbPh_3$ (3)

A toluene solution of 4,5-dichloro-3,6-di-*tert*-butyl-*o*-benzoquinone (100 mg, 0.34 mmol, 20 ml of toluene) was added with stirring to a toluene solution of triphenylstibine (120 mg, 0.34 mmol, 20 ml of toluene) over a period of 10 min. After the addition was complete, the reaction mixture became yellow. Removal of solvent under vacuum yielded a solid material. Recrystallization of this crude material from the appropriate solvent (see below) yielded microcrystalline product **3** (195 mg, 89%).

Elemental analysis calcd (%) for $C_{32}H_{33}Cl_2O_2Sb$ (642 g mol^{-1}): C 59.81, H 5.18, Cl 11.04, Sb 18.96; found: C 59.68, H 5.11, Cl 10.99, Sb 18.98.

IR (Nujol, ῡ, cm^{-1}): 1610 m, 1578 m, 1478 s, 1463 s, 1433 s, 1397 s, 1370 s, 1303 m, 1245 s, 1214 s, 1187 m, 1155 m, 1068 m, 1062 m, 1032 m, 1021 m, 997 m, 978 s, 927 m, 917 m, 838 s, 775 s, 730 s, 693 s, 674 m, 656 m, 633 m, 590 w, 552 w, 500 m, 452 s.

^{1}H NMR ($CDCl_3$, 293 K, δ/ppm, J/Hz): 1.64 (s, 18H, *t*-Bu), 7.4–7.54 (m, 9H, o-, p-H, 3Ph), 7.66–7.78 (m, 6H, m-H, Ph).

^{13}C{^{1}H} NMR ($CDCl_3$, ppm): 32.24 (CH_3, *t*-Bu), 38.52 (C, *t*-Bu), 128.87 (Ar), 129.31 (*m*-C, $SbPh_3$), 131.34 (*p*-C, $SbPh_3$), 134.77 (*o*-C, $SbPh_3$), 136.24 (*i*-C, $SbPh_3$), 137.23 (C–Cl, Ar), 145.57 (CO).

2.2.2. (4-(2,6-Dimethylphenyliminomethyl)pyridine) (3,6-di-tert-butyl-catecholato)-triphenylantimony(V) (3,6-DBCat)$SbPh_3$·(Py-CH=N–Ar) (4)

A solution of (3,6-di-*tert*-butyl-catecholato)triphenylantimony(V) (**1**), (257 mg, 0.45 mmol) in toluene (20 mL) was added to a stirred solution of 4-(2,6-dimethylphenyliminomethyl)pyridine (119 mg, 0.45 mmol) in toluene (15 mL). The reaction was allowed to proceed over half an hour at room temperature, during which time the mixture gradually changed color from cherry red to orange. The resulting solution was concentrated to 15 mL and stored for a day at 0 °C. The product **4** was isolated by filtration and recrystallized over a longer period from toluene to yield yellow crystalline sample of **4** (260 mg, yield is 69%);

Elemental analysis calcd (%) for $C_{50}H_{57}N_2O_2Sb$ (839 g mol^{-1}): C 71.51, H 6.79, Sb 14.51; found: C 71.28, H 6.51, Sb 14.40.

IR (Nujol, cm^{-1}): ῡ = 1650 w, 1632 s, 1606 s, 1580 m, 1557 m, 1416 s, 1401 s, 1377 s, 1355 s, 1318 s, 1306 s, 1282 s, 1262 s, 1241 s, 1200 s, 1173 s, 1161 m, 1144 s, 1106 m, 1096 m, 1075 s, 1063 m, 1057 s, 1023 m, 1004 s, 998 m, 977 s, 941 s, 925 m, 884 m, 848 m, 827 m, 801 m, 789 s, 762 s, 733 s, 727 s, 694 s, 661 m, 658 m, 648 s, 628 m, 601 m, 559 w, 547 w, 540 w, 526 m, 510 w, 464 s, 454 s.

^{1}H NMR ($CDCl_3$, 293 K, δ/ppm, J/Hz): 1.18 (d, 6.8 Hz, 12H, *i*-Pr), 1.43 (s, 18H, *t*-Bu), 2.90 (sept, 6.8 Hz, 2 H, CH, *i*-Pr), 6.62 (s, 2H, arom. C_6H_2), 7.17 (m, 3H, arom. C_6H_3), 7.38–7.55 (m, 9H, *o*-,*p*-H of Ph), 7.70–7.86 (m, 8H: 6 *m*-H of Ph and 2H of Py), 8.20 (s, 1H, CH=N), 8.78 (d, 4.1 Hz, 2 H of Py).

^{13}C{^{1}H} NMR ($CDCl_3$, δ/ppm): 23.39 (CH_3, iPr), 28.02 (CH, iPr), 29.58 (CH_3, *t*-Bu), 34.15 (C, *t*-Bu), 114.24, 122.14, 123.16, 124.75, 129.07 (*m*-C, $SbPh_3$), 130.94 (*p*-C, $SbPh_3$), 132.14, 135.02 (*o*-C, $SbPh_3$), 137.16 (*i*-C, $SbPh_3$), 138.48, 142.57, 145.34, 148.46 (C–O), 150.54, 160.24 (CH=N).

2.2.3. (4-(2,6-Dimethylphenyliminomethyl)pyridine) (4,5-(N,N′-piperazine-1,4-diyl)-3,6-di-tert-butyl-catecholato) triphenylantimony(V) (4,5-pip-3,6-DBCat)$SbPh_3$·(Py-CH = N–Ar) (5)

The pure sample of complex **5** was obtained from 100 mg (0.15 mmol) of (4,5-(*N,N′*-piperazine-1,4-diyl)-3,6-di-*tert*-butyl-catecholato)triphenylantimony(V) (**2**) and 4-(2,6-dimethylphenyliminomethyl)pyridine (41 mg, 0.15 mmol) by the same method as described for complex **4**. The yield of **5** is 129 mg (72%).

Elemental analysis calcd (%) for $C_{54}H_{63}N_4O_2Sb$ (921 g mol^{-1}): C 70.36, H 6.84, Sb 13.25; found: C 70.28, H 6.71, Sb 13.28.

IR (Nujol, ῡ, cm^{-1}): 1652 w, 1638 s, 1606 s, 1561 m, 1477 s, 1433 s, 1414 m, 1377 s, 1345 m, 1334 m, 1318 m, 1297 m, 1275 m, 1260 m, 1234 s, 1225 s, 1202 m, 1175 m, 1109 w, 1092 w, 1072 m, 1059 m, 1052 m, 1038 s, 1023 m, 995 s, 986 s, 934 s, 886 w, 870 w, 854 m, 825 m, 796 m, 773 m, 758 m, 732 s, 696 s, 658 m, 628 w, 594 w, 561 m, 520 m, 461 s.

^{1}H NMR ($CDCl_3$, 293 K, δ/ppm, J/Hz): 1.18 (d, 6.8 Hz, 12H, CH_3, *i*-Pr), 1.61 (s, 18H, *t*-Bu), 2.55–3.10 (m, 10H, 2 CH of *i*-Pr and 8 H of $N(CH_2CH_2)_2N$), 7.17 (m, 3H, arom. C_6H_3), 7.35–7.55 (m, 9H, *o*-, *p*-H of Ph), 7.65–7.85 (m, 8H, *m*-H of Ph; 2H of Py), 8.20 (s, 1H, CH=N), 8.79 (d, 5.1 Hz, 2H of Py).

^{13}C{^{1}H} NMR ($CDCl_3$, δ/ppm): 11.40, 14.08, 18.75, 22.64, 23.39, 28.03, 25.29, 28.03, 29.06, 30.73, 31.58, 32.35, 34.51, 34.68, 35.47, 50.17, 122.07, 123.15, 124.74, 128.53, 129.0 (m-C, $SbPh_3$), 130.89 (p-C, $SbPh_3$), 135.08 (o-C, $SbPh_3$), 137.16, 138.30, 141.13, 142.51, 143.67, 148.49 (C–O), 150.68, 160.29 (C=N).

2.2.4. (4-(2,6-Dimethylphenyliminomethyl)pyridine) (4,5-dichloro-3,6-di-tert-butyl-catecholato)triphenylantimony(V) (4,5-Cl_2-3,6-DBCat)$SbPh_3$·(Py-CH = N–Ar) (6)

Complex **6** was obtained by the same method as described for complex **4** from 100 mg (0.15 mmol) of (4,5-dichloro-3,6-di-*tert*-butylcatecholato)-triphenylantimony(V) (**3**) and 41 mg (0.15 mmol) of 4-(2,6-dimethylphenyliminomethyl)pyridine. Yield of **7** is 99 mg (70%).

Elemental analysis calcd (%) for $C_{50}H_{55}N_2Cl_2O_2Sb$ (908 g mol^{-1}): C 66.08, H 6.06, Sb 13.44; found: C 66.10, H 6.04, Sb 13.44.

IR (Nujol, ῡ, cm^{-1}): 1656 w, 1636 s, 1610 s, 1578 m, 1558 m, 1478 s, 1431 s, 1417 m, 1395 s, 1365 s, 1316 s, 1266 m, 1250 s, 1233 m, 1202 s, 1182 s, 1159 m, 1112 m, 1092 m, 1071 m, 1065 m, 1059 m, 1042 m, 1028 m, 1006 m, 998 m, 980 s, 970 m, 930 m, 885 m, 835 s, 796 m, 772 s, 759 s, 733 s, 693 s, 668 m, 658 m, 630 m, 617 w, 590 w, 559 w, 546 w, 532 w, 513 m, 494 m, 461 s, 453 m.

^{1}H NMR ($CDCl_3$, 293 K, δ/ppm, J/Hz): 1.18 (d, 6.8 Hz, 12H, CH_3, *i*-Pr), 1.64 (s, 18H, *t*-Bu), 2.90 (sept., 6.8 Hz, 2H, CH, iPr), 7.18 (m, 3H, C_6H_3), 7.40–7.58 (m, 9H, *o*-, *p*-H, Ph), 7.66–7.80 (m, 8H: 6 *m*-H, Ph; 2H, Py), 8.20 (s, 1H, CH=N), 8.70 (d, 5.1 Hz, 2H, Py).

^{13}C{^{1}H} NMR ($CDCl_3$, ppm): 23.38 (CH_3, i-Pr), 28.0 (CH, iPr), 32.26 (CH_3, *t*-Bu), 38.51(C, *t*-Bu), 122.12, 123.15,123.54, 124.78, 128.58, 128.85, 129.16 (*m*-C, $SbPh_3$), 129.7, 131,03 (*p*-C, $SbPh_3$), 134.75(*o*-C, $SbPh_3$), 136.22 (i-C, $SbPh_3$), 137.13, 138.28, 142.75, 145.73, 148.41 (C–O), 150.35, 160.08 (CH=N).

2.2.5. Tetraphenylstibonium(V) bis-(4,5-dichloro-3,6-di-tert-butylcatecholato)-diphenylantimonate(V) $[Ph_4Sb]^+[(4,5\text{-}Cl_2\text{-}3,6\text{-}DBCat)_2SbPh_2]^-$ (7)

A sample of triphenylantimony(V) catecholate **3** (100 mg) was dissolved in acetonitrile (30 ml) and heated at 60 °C for three days. Then 20 ml of toluene was added, and the resulting solution was stored at ambient temperature for 1 week. The X-ray quality crystals **7**·0.5toluene formed (65 mg), they were collected and dried on air. The yield is 62.7%.

Elemental analysis calcd (%) for $C_{67.5}H_{70}Cl_4O_4Sb_2$, **7**·0.5toluene, (1330.5 g mol^{-1}): C 60.93, H 5.30, Cl 10.66, Sb 18.30; found: C 60.69, H 5.20, Cl 10.41, Sb 18.15.

^{1}H NMR (CD_3CN, 295 K, δ/ppm): 1.29 (s, 18H, *t*-Bu), 1.62 (s, 18H, *t*-Bu), 7.24–7.36 (m, 4H, Ph), 7.51–7.62 (m, 4H, Ph), 7.62–7.80 (m, 20H, $SbPh_4$), 8.10–8.25 (m, 2H, Ph).

^{13}C{^{1}H} NMR (CD_3CN, δ/ppm): 32.46 (CH_3, *t*-Bu), 32.76 (CH_3, *t*-Bu), 39.15 (C, *t*-Bu), 39.34 (C, *t*-Bu), 129.05 (*m*-C, $SbPh_2$), 129.48, 129.66, 129.91, 130.09, 130.36 (*p*-C, $SbPh_2$), 131.95 (*m*-C, $SbPh_4$), 134.28 (*o*-C, $SbPh_2$), 134.65 (*p*-C, $SbPh_4$), 135.28 (*i*-C, $SbPh_2$), 135.35 (*i*-C, $SbPh_4$), 136.66 (*o*-C, $SbPh_4$), 143.20 (C–O), 145.16 (C–O).

2.2.6. (3,6-Di-tert-butyl-catecholato)-pyridine-triphenylantimony(V) (3,6-DBCat)$SbPh_3$·Py (8)

Pyridine (0.020 ml, 0.248 mmol) was added with a micropipette to the toluene solution of (3,6-di-*tert*-butyl-catecholato)triphenylantimony(V) (**1**) (100 mg, 0.175 mmol, toluene 20 mL). The reaction mixture was stirred for an hour at room temperature. The resulting solution was concentrated to 10 mL and stored for a day at room temperature. The pale yellow powder precipitated. The product **8** was isolated by filtration and dried on air. The yield of **8** is 88 mg (77%).

Elemental analysis calcd (%) for $C_{37}H_{40}NO_2Sb$ (652 g mol^{-1}): C 68.11, H 6.18, Sb 18.66; found: C 68.22, H 6.23, Sb 18.39.

IR (Nujol, cm^{-1}): ῡ = 1595 m, 1584 w, 1577 w, 1541 w, 1480 s, 1443 s, 1433 s, 1408 s, 1353 m, 1311 m, 1285 s, 1269 s, 1243 s, 1214 s, 1205 w, 1199 w, 1183 w, 1147 m, 1067 s, 1036 m, 1025 m, 1003 m, 997 m, 979 s, 944 s, 928 m, 875 w, 849 w, 812 m, 794 s, 753 s, 733 s, 730 s, 696 s, 659 w, 649 w, 623 m, 601 w, 551 w, 463 s.

^{1}H NMR ($CDCl_3$, 293 K, δ/ppm, J/Hz): 1.43 (s, 18H, *t*-Bu), 6.61 (s, 2H, arom. C_6H_2), 7.20–7.30 (m, 2H of Py), 7.37–7.53 (m, 9H, *o*-,*p*-H of Ph), 7.62–7.72 (m, 1H of Py), 7.74–7.85 (m, 6 *m*-H of Ph), 8.55 (d, 4.4 Hz, 2 H of Py).

^{13}C{^{1}H} NMR ($CDCl_3$, δ/ppm): 29.55 (CH_3, *t*-Bu), 34.12 (C, *t*-Bu), 114.11, 123.74, 128.58 (*m*-C, $SbPh_3$), 130.78 (*p*-C, $SbPh_3$), 132.08 (*o*-C, $SbPh_3$), 134.99, 136.29, 138.93 (*i*-C, $SbPh_3$), 145.39 (C–O), 149.44.

2.3. X-ray diffraction

X-ray suitable crystals of complexes **3**, **4** and **5** were obtained from the mixture hexane-toluene (the mixture 2:1 vol for **3** and 1:1 vol for **4** and **5**), **6** – from toluene, and **7** – from a mixture toluene-acetonitrile (2:3).

X-ray diffraction intensity data for compounds **3**–**7** were collected at 100 K on *Agilent Xcalibur E* (**3**, **4**, **6**, **7**) and *Smart Apex I* (**5**) diffractometers with graphite monochromated *Mo-*K_α radiation (λ = 0.71073 Å) using ω scans. The structures were solved by direct methods and were refined on F^2 using *SHELXTL* [18] and *Crysalis Pro* [19] packages. All non-hydrogen atoms in **3**–**7** were refined anisotropically. The H atoms were placed in calculated positions and were refined in the riding model with $U_{iso}(H) = 1.2\ U_{eq}$ and $U_{iso}(H) = 1.5\ U_{eq}$ for the hydrogen atoms of their parent atoms. *SADABS* [20] and *ABSPACK (Crysalis Pro)* [19] were used to perform area-detector scaling and absorption corrections. The single crystals of **6** have the poor quality and weak diffraction. Crystal data and details of data collection and structure refinement for the different compounds are given in Table 1. The CCDC 1875551 (**3**), 1875552 (**4**), 1875553 (**5**·1.6n-hexane), 1875554 (**6**) and 1875555 (**7**·0.5toluene) contain the supplementary crystallographic data for this paper. These data can be obtained free of charge via ccdc.cam.ac.uk/community/requestastructure.

2.4. Electrochemistry

Electrochemical studies were carried out using IPC-Pro potentiostate in three-electrode mode. The stationary glassy carbon (d = 2 mm) disk was used as working electrode; the auxiliary electrode was a platinum-flag electrode. The reference electrode was a Ag/AgCl/KCl (sat.) with watertight diaphragm and ferrocene was added as internal standard ($E_{1/2}(Fc^+/Fc) = 0.51$ V vs. Ag/AgCl/KCl(sat.)). All measurements were carried out under argon. The samples were dissolved in the pre-deaerated solvent. The rate scan was 200 mV s^{-1}. The supporting electrolyte 0.1 M Bu_4NClO_4 (99%, "Acros") was undergone twice recrystallization from aqueous EtOH and then it was dried in vacuum (48 h) under 50 °C. The compounds **3**–**6** and **8** show linear dependencies of the first anodic current peaks with the square root of the scan rate ($v^{1/2}$) indicating a diffusion controlled system in the range of potential sweep from 0.05 to 1.00 V s^{-1}.

In order to determine a number of electrons transferred in electrode processes, microelectrolysis of complexes **4**, **6** and **8** was performed using potentiostate "VersaSTAT-3" at 25°C in a diaphragmless three-electrode cell at controlled-potential conditions (E = 1.1 V). The platinum flag electrodes with the surface area of 0.7 cm^2 were applied. The coulometric measurements have shown that the amounts of transmitted electricity in microelectrolysis were 2.0–2.1 F/mol.

3. Results and discussion

3.1. Synthesis and characterization

As it was shown previously, the initial pentacoordinated triphenylantimony(V) catecholates (3,6-DBCat)$SbPh_3$ (**1**) and (4,5-pip-3,6-DBCat)$SbPh_3$ (**2**) (Scheme 1) have the tendency to increase the coordination number to six either through the intermolecular interactions between neighboring complex molecules or via the coordination of solvents such as methanol, acetonitrile etc [3b,16]. In the course of this study we have synthesized triphenylantimony(V) 4,5-dichloro-3,6-di-*tert*-butyl-catecholate complex (4,5-Cl_2-3,6-DBCat)$SbPh_3$ (**3**) containing electron-withdrawing chlorine substituents in the aromatic ring of catecholate ligand. Complex **3** was isolated from a hexane-toluene (2:1) solution as yellow-orange crystals suitable for single crystal X-ray analysis. In crystal of **3**, the additional intermolecular interaction between one of two chlorine atoms in Cat ligand of one complex molecule and the central antimony atom of another molecule was observed leading to the fulfilling the antimony(V) coordination sphere and to the formation of 1D polymeric structure (see part 3.2).

Table 1
Crystallographic and refinement data for **3**, **4**, **5**·1.6n-hexane, **6**, **7**·0.5toluene.

Complex	3	4	5·1.6n-hexane	6	7·0.5toluene
Empirical formula	$C_{32}H_{33}Cl_2O_2Sb$	$C_{50}H_{57}N_2O_2Sb$	$C_{63.6}H_{85.4}N_4O_2Sb$	$C_{50}H_{55}Cl_2N_2O_2Sb$	$C_{67.50}H_{70}Cl_4O_4Sb_2$
Formula weight	642.23	839.72	1059.70	908.61	1330.53
T/K	100 (2)	100 (2)	100 (2)	100 (2)	100 (2)
Crystal system	Monoclinic	Monoclinic,	Triclinic	Monoclinic	Monoclinic
Space group	P2 (1)/n	P2 (1)/n	P-1	P2/c	P2 (1)/n
a/Å	10.46407 (15)	16.9251 (2)	14.0502 (6)	43.6526 (11)	12.78510 (10)
b/Å	13.78279 (19)	14.48910 (10)	14.6311 (7)	10.35473 (14)	34.3294 (4)
c/Å	19.9636 (3)	18.9547 (2)	14.9242 (7)	20.2919 (4)	13.71590 (10) A
α/deg	90	90	72.3930 (10)	90	90
β/deg	96.9271 (14)	105.7390 (10)	73.3120 (10)	102.911 (2)	91.3600 (10)
γ/deg	90	90	86.0330 (10)	90	90
V/Å^3	2858.22 (7)	4473.97 (8)	2800.6 (2)	8940.3 (3)	6018.28 (10)
Z	4	4	2	8	4
ρ/g cm^{-3}	1.492	1.247	1.257	1.350	1.468
μ/mm^{-1}	1.180	0.656	0.539	0.778	1.123
F (000)	1304	1752	1124	3760	2708
Crystal size/mm	0.300 × 0.250 x 0.200	0.400 × 0.200 x 0.200	0.400 × 0.350 x 0.220	0.300 × 0.200 x 0.050	0.856 × 0.278 x 0.167
θ range for data collection/deg	2.956–32.652	3.025–30.435	1.803–27.999	2.964–25.000	3.030–28.999
Limiting indices	−15 ≤ h<=13	−24 ≤ h<=24	−18 ≤ h<=18	−51 ≤ h<=51	−17 ≤ h<=17
	−20 ≤ k<=20	−20 ≤ k<=20	−19 ≤ k<=19	−12 ≤ k<=12	−46 ≤ k<=46
	−29 ≤ l<=29	−27 ≤ l<=27	−19 ≤ l<=19	−24 ≤ l<=24	−18 ≤ l<=18
Refls. collected	35748	98939	28361	70907	112046
Unique refls. collected	9683	13536	13397	15723	15979
R_{int}	0.0514	0.0318	0.0202	0.0808	0.0387
Data/restraints/parameters	9683/0/340	13536/43/525	13397/166/705	15723/1020/1018	15979/102/799
Goodness-of-fit on F^2	1.029	1.031	1.050	1.075	1.065
R_1/wR_2 ($I > 2\sigma(I)$)	0.0350/0.0662	0.0513/0.1494	0.0349/0.0848	0.1182/0.2746	0.0411/0.0831
R_1/wR_2 (all data)	0.0595/0.0755	0.0536/0.1507	0.0388/0.0874	0.1235/0.2792	0.0463/0.0848
Largest diff. peak and hole/e•Å^{-3}, ρ_{max}/ρ_{min}	0.869/−1.002	1.078/−1.592	1.056/−0.647	2.463/−3.189	0.705/−1.473

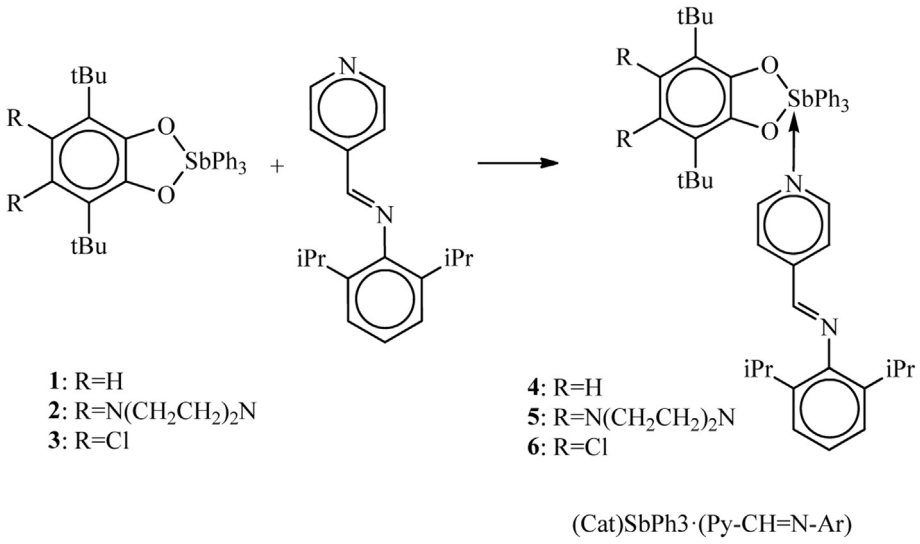

Scheme 1. The preparation of complexes **4-6** from **1-3**.

We have investigate the reactions of The interaction of triphenylantimony(V) 3,6-di-*tert*-butyl-catecholate (**1**), 4,5-(*N*,*N*'-piperazine-1,4-diyl)-3,6-di-*tert*-butyl-catecholate (**2**) and 4.5-dichloro-3,6-di-*tert*-butyl-catecholate (**3**) with 4-(2,6-dimethylphenyliminomethyl)pyridine (Py-CH═N–Ar) in toluene leads to the coordination of pyridine group to the central antimony atom with the formation of corresponding complexes **4**–**6** of the common type (Cat)$SbPh_3$·(Py-CH═N–Ar) (Scheme 1).

Triphenylantimony(V) 4,5-dichloro-3,6-di-*tert*-butylcatecholate (4,5-Cl_2-3,6-DBCat)$SbPh_3$ (**3**) is stable in such solvents as toluene, benzene, however **3** undergoes a slow rearrangement under heating in a mixture of polar solvents acetonitrile-methanol to form ionic derivative $[Ph_4Sb]^+[(4,5\text{-}Cl_2\text{-}3,6\text{-}DBCat)_2SbPh_2]^-$ (**7**) containing tetraphenylstibonium(V) cation and bis-catecholato-diphenylantimony(V) anion (Scheme 2). 3,6-Di-*tert*-butyl-catecholate **1** and its piperazine-substituted analog **2** do not undergo such transformation in polar solvents [14,16]. However, earlier it was found that other types of triphenylantimony(V) catecholates (for example, phenanthrene-9,10-diolato)triphenylantimony(V) [3a] or (4,5-(1,1,4,4-tetramethyl-butane-1,4-diyl)-catecholato)triphenylantimony(V) [21]) undergo such rearrangement with a formation of related ionic compounds of the type $[Ph_4Sb]^+[Cat_2SbPh_2]^-$.

Complex **7** was isolated as X-ray quality crystalline material (see

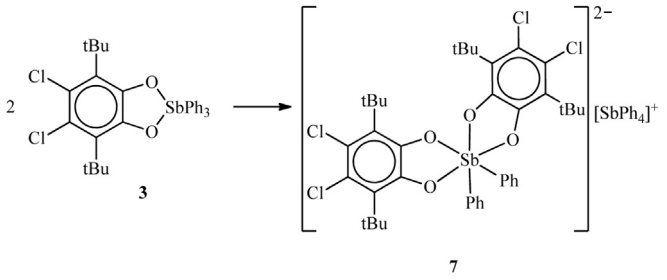

Scheme 2. Rearrangement of 3 to ionic complex **7**.

part 3.2) from the mixture toluene-acetonitrile.

Starting from **1** and unsubstituted pyridine we have synthesized complex with coordinated pyridine ligand - (3,6-DBCat)$SbPh_3 \cdot Py$ (**8**) - in order to compare its electrochemical behaviour with the electrochemical behaviour of iminopyridine-containing complexes **4**–**6**.

The composition and structures of the synthesized compounds **3**–**8** have been determined by means of IR, ^1H and ^{13}C NMR spectroscopy, elemental analysis and single-crystal X-ray analysis (**3**–**7**).

The IR spectra of the obtained complexes contain the intense absorption bands in the region of 1640–1580 cm^{-1} characteristic for double and aromatic bonds C=N [22], in the region of 1400–1180 cm^{-1} - for single C–O and C–N bonds. The IR spectra also contain valence vibrations of Sb-C_{Ph} bonds in the region of 510–450 cm^{-1}, Sb–O - 620-650 cm^{-1}, deformation vibrations of $SbPh_3$ fragment at 930-690 cm^{-1}.

The ^1H NMR spectra of the synthesized catecholates **4**–**6** have common features such as singlet from the equivalent *tert*-butyl groups in the region of 1.43 (for **4**) and 1.61–1.64 (for **5** and **6**) ppm, the doublet from CH_3 groups and the multiplet from CH protons of isopropyl substituents of 4-(2,6-diisopropylphenyliminomethyl) pyridine ligand in the region of 1.18 and 2.8–3.0 ppm respectively, two multiplets from aromatic protons in triphenylantimony(V) in the region of 7.40–7.84 ppm. At the same time, ^1H NMR spectra of complexes **4**–**6** have the differences due to the presence or absence of substituents in the 4th and 5th positions of 3,6-di-*tert*-butylcatecholate ligand: the presence of a singlet at 6.62 ppm from two protons of 3,6-di-*tert*-butylcatecholate ligand to complex **4**, and its absence in the spectra of complexes **5** and **6**; a multiplet from methylene protons of piperazine groups in the region 2.55–3.10 ppm for complex **5**.

3.2. X-ray structures

X-ray suitable crystals of complexes **3**, **4** and **5** were obtained from the mixture hexane-toluene (the mixture 2:1 vol for **3** and 1:1 vol for **4** and **5**), **6** – from toluene, and **7** – from a mixture toluene-acetonitrile (2:3). Crystals of piperazine-substituted catecholate **5** contain 1.6 solvated molecules of n-hexane per each complex molecule (**5**·1.6n-hexane), the crystals of **7** contain 0.5 solvated toluene molecule per each complex molecule (**7**·0.5toluene). The unit cell of **6** contains two independent molecules of complex. The selected bond lengths and angles for complexes **3** and **7** are given in Table 2, **4**–**6** – in Table 3.

The molecular structure of **3** in crystals is shown on Fig. 1.

In molecule of **3**, the central atom Sb(1) disposes in a distorted

Table 2
The selected bond distances and angles for **3** and **7**.

3		**7**			
Bond	d/Å	Bond	d/Å	Bond	d/Å
Sb(1)–O (1)	2.029 (2)	Sb(1)–O (1)	2.052 (2)	Sb(1)–C (29)	2.139 (3)
Sb(1)–O (2)	2.035 (2)	Sb(1)–O (2)	2.020 (2)	Sb(1)–C (35)	2.145 (3)
Sb(1)–C (15)	2.128 (2)	Sb(1)–O (3)	2.023 (2)	Sb(2)–C (41)	2.099 (3)
Sb(1)–C (21)	2.135 (2)	Sb(1)–O (4)	2.013 (2)	Sb(2)–C (47)	2.091 (3)
Sb(1)–C (27)	2.109 (2)			Sb(2)–C (53)	2.091 (3)
				Sb(2)–C (59)	2.094 (3)
C (1)–O (1)	1.359 (2)	C (1)–O (1)	1.341 (3)	C (15)–O (3)	1.355 (3)
C (2)–O (2)	1.360 (2)	C (2)–O (2)	1.362 (3)	C (16)–O (4)	1.355 (3)
C (1)–C (2)	1.409 (3)	C (1)–C (2)	1.427 (4)	C (15)–C (16)	1.425 (4)
C (1)–C (6)	1.402 (3)	C (1)–C (6)	1.408 (4)	C (15)–C (20)	1.402 (4)
C (2)–C (3)	1.405 (3)	C (2)–C (3)	1.405 (4)	C (16)–C (17)	1.405 (4)
C (3)–C (4)	1.413 (3)	C (3)–C (4)	1.413 (4)	C (17)–C (18)	1.409 (4)
C (4)–C (5)	1.406 (3)	C (4)–C (5)	1.394 (4)	C (18)–C (19)	1.397 (5)
C (5)–C (6)	1.414 (3)	C (5)–C (6)	1.414 (4)	C (19)–C (20)	1.411 (5)
Cl (1)–C (4)	1.746 (2)	Cl (1)–C (4)	1.752 (3)	Cl (3)–C (18)	1.750 (3)
Cl (2)–C (5)	1.752 (2)	Cl (2)–C (5)	1.751 (3)	Cl (4)–C (19)	1.754 (3)
Angle	ω/°	Angle	ω/°	Angle	ω/°
O (1)-Sb(1)-O (2)	77.16 (6)	O (1)-Sb(1)-O (2)	78.68 (8)	O (1)-Sb(1)-C (35)	168.50 (10)
O (1)-Sb(1)-C (27)	100.00 (7)	O (1)-Sb(1)-O (3)	83.51 (8)	O (2)-Sb(1)-C (35)	91.40 (9)
O (2)-Sb(1)-C (27)	97.52 (8)	O (1)-Sb(1)-O (4)	91.53 (8)	O (3)-Sb(1)-C (35)	90.72 (10)
O (1)-Sb(1)-C (15)	86.30 (7)	O (2)-Sb(1)-O (3)	89.72 (8)	O (4)-Sb(1)-C (35)	97.25 (10)
O (2)-Sb(1)-C (15)	153.20 (7)	O (2)-Sb(1)-O (4)	166.54 (8)	C (29)-Sb(1)-C (35)	98.70 (11)
C (27)-Sb(1)-C (15)	106.10 (9)	O (3)-Sb(1)-O (4)	79.93 (8)	C (47)-Sb(2)-C (53)	111.84 (12)
O (1)-Sb(1)-C (21)	150.01 (7)	O (1)-Sb(1)-C (29)	88.64 (10)	C (47)-Sb(2)-C (59)	107.83 (11)
O (2)-Sb(1)-C (21)	85.21 (7)	O (2)-Sb(1)-C (29)	98.77 (10)	C (53)-Sb(2)-C (59)	107.98 (11)
C (27)-Sb(1)-C (21)	106.28 (9)	O (3)-Sb(1)-C (29)	167.12 (10)	C (41)-Sb(2)-C (47)	110.53 (11)
C (15)-Sb(1)-C (21)	99.81 (8)	O (4)-Sb(1)-C (29)	90.12 (10)	C (41)-Sb(2)-C (53)	108.70 (12)
				C (41)-Sb(2)-C (59)	109.92 (12)

Table 3
The selected bond lengths (Å) and angles (°) in **4** and **5**.

4		**5**	
Bond	d/Å	Bond	d/Å
Sb(1)–O (1)	2.031 (2)	Sb(1)–O (1)	2.021 (2)
Sb(1)–O (2)	2.039 (2)	Sb(1)–O (2)	2.035 (2)
Sb(1)–C (33)	2.148 (3)	Sb(1)–C (37)	2.137 (2)
Sb(1)–C (39)	2.151 (3)	Sb(1)–C (43)	2.141 (2)
Sb(1)–C (45)	2.143 (3)	Sb(1)–C (49)	2.144 (2)
Sb(1)–N (1)	2.509 (2)	Sb(1)–N (3)	2.576 (2)
C (1)–O (1)	1.357 (3)	C (1)–O (1)	1.359 (2)
C (2)–O (2)	1.362 (3)	C (2)–O (2)	1.365 (2)
N (2)–C (20)	1.264 (5)	N (4)–C (24)	1.267 (3)
N (2)–C (21)	1.419 (4)	N (4)–C (25)	1.428 (2)
C (1)–C (2)	1.407 (4)	C (1)–C (2)	1.425 (2)
C (1)–C (6)	1.404 (4)	C (1)–C (6)	1.404 (3)
C (2)–C (3)	1.406 (4)	C (2)–C (3)	1.403 (2)
C (3)–C (4)	1.404 (4)	C (3)–C (4)	1.410 (3)
C (4)–C (5)	1.388 (4)	C (4)–C (5)	1.390 (3)
C (5)–C (6)	1.406 (4)	C (5)–C (6)	1.409 (3)
4		**5**	
Angle	ω/°	Angle	ω/°
O (1)-Sb(1)-O (2)	79.27 (8)	O (1)-Sb(1)-O (2)	78.45 (5)
O (2)-Sb(1)-C (33)	162.09 (9)	O (2)-Sb(1)-C (43)	161.44 (6)
O (1)-Sb(1)-C (39)	158.02 (10)	O (1)-Sb(1)-C (49)	156.42 (7)
C (45)-Sb(1)-N (1)	177.46 (9)	C (37)-Sb(1)-N (3)	173.31 (6)

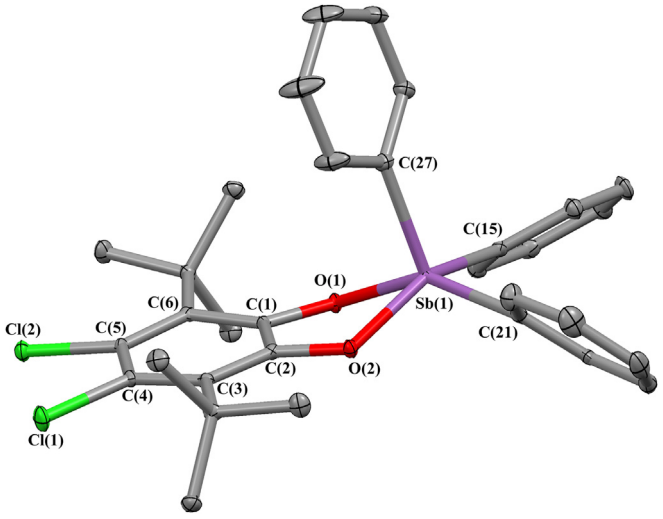

Fig. 1. The molecular structure of (4,5-Cl_2-3,6-DBCat)$SbPh_3$ (**3**) in crystals (ellipsoids of 30% probability). The hydrogen atoms are omitted.

tetragonal pyramidal environment with the base formed by oxygen atoms O (1) and O (2) of catecholato ligand and carbons C (15), C (21) of two phenyl groups. The metallocycle in **3** is not planar, the torsion angle O (1)C (1)C (2)O (2) is 4.25°, the bending angle along O (1) … O (2) line is 23.10°. The aromatic ring C (1–6) is also distorted due to the staggered conformation of *tert*-butyl groups.

The apical bond Sb(1)–C (27) of 2.109 (2) Å is slightly shorter than the equatorial bonds Sb(1)–C (15) and Sb(1)–C (21) (2.128 (2) and 2.135 (2) Å, respectively). The bond angles O (2)-Sb(1)-C (15) and O (1)-Sb(1)-C (21) are close (153.20 (7) and 150.01 (7)°, respectively).

The parameter describing pentacoordinated compounds $\tau = 0.053$ meaning that the coordination polyhedron may be described as a distorted tetragonal pyramid. However, in crystal the additional intermolecular contacts between chlorine atom Cl (2) of one complex molecule with the central antimony atom Sb(1) of another complex molecule are observed. The distance Sb(1) … Cl (2) are 3.457 (2) Å that is shorter than the sum of Van-der-Waals radii of these elements (2.2 + 1.8 = 4.0 Å [23]). Thus, the coordination number of Sb(1) increases to six. The molecules of **3** are situated in crystal is such a way that they form 1D coordination chains (Fig. 2). It is worthy of note that the crystal packing motif of **3** differs significantly from packing motifs for complex **1** [3b]. The solid-state structure of **1** contain "dimeric" packing motif. In crystal, complex (3,6-DBCat)$SbPh_3$ has square-pyramidal geometry and packs in a "back-to-back" fashion with the bases of the pyramids facing each other. In the case of complex **2** it was crystallized only as a hexacoordinated antimony(V) complex **2**·MeOH with a coordinated methanol molecule [16].

The molecular structures of complexes **4**, **5** and **6** in crystal state are shown in Fig. 3. The coordination environment of the central antimony atom in **4**–**6** is a distorted octahedron with the equatorial plane formed by oxygen atoms O (1), O (2) of the chelating catecholate ligand and atoms with two phenyl substituents. The apical positions are occupied by the nitrogen atom of the pyridine fragment (atom N (1) in **4** and **6**, and N (3) in **5**) and carbon atom of the third phenyl group (atom C (45) in **3**, C (37) in **4**, and C (21) in **5**).

The quality of crystals of **6** was poor and therefore in order to avoid some speculative discussion we will compare the X-ray data of complexes **4** and **5**. The deviation of the central antimony atom Sb(1) from the octahedron base plane is 0.290 Å for **4** and 0.312 Å for **5**. The deviation of Sb(1) from the plane of catecholate ligand formed by atoms C (1)–C (6), O (1), O (2) is 0.198 Å for **4**, 0.455 Å for **5**. The Sb(1)–O (1) and Sb(1)–O (2) bond lengths (Table 3) are typical for antimony(V) catecholates [3,24,25]. The bond length between antimony and nitrogen atom of pyridine group Sb(1)–N (1) in **4** is 2.509 (2) Å, Sb(1)–N (3) in **5** is 2.576 (16) Å. These bond distances are some longer than the sum of covalent radii of the corresponding elements (1.43 + 0.74 = 2.17 Å) [23], however they are significantly less than the sum of the corresponding van der Waals radii (2.2 + 1.6 = 3.8 Å) [23]. Thus, these Sb–N distances correspond to the donor-acceptor binding. It should be noted that the distance Sb-N_{Py} shortens in the row (4,5-pip-3,6-DBCat) $SbPh_3$·(Py-CH=N–Ar) (**5**), (3,6-DBCat)$SbPh_3$·(Py-CH=N–Ar) (**4**), (4,5-Cl_2-3,6-DBCat)$SbPh_3$·(Py-CH=N–Ar) (**6**) meaning the increasing donor-acceptor bonding Sb–N with the increasing electron-withdrawing properties of catecholato ligand.

Metallocycles Sb(1)O (1)C (1)C (2)O (2) in complexes are not planar. The torsion angle O (1)C (1)C (2)O (2) in **4** is 0.43°, in **5**–3.02°. The bend angle along the line O (1) ….O (2) - 8.33° (in **4**), 18.90° (in **5**), respectively. These differences are due to the fact that the presence of the piperazine group in **5** leads to a reversal orders of *tert*-butyl substituents in eclipsed conformation: the methyl groups of tert-butyls facing the central antimony atom lie in the plane of the catecholate ligand, thereby increasing the steric tension in the metal cycle.

The X-ray structure of complex **7** is shown on Fig. 4. The selected bond lengths and angles are listed in Table 2. The Sb(1) atom in complex anion $[(4,5\text{-}Cl_2\text{-}3,6\text{-}DBCat)_2SbPh_2]^-$ adopts the distorted octahedral environment, and Sb(2) in cation $[Ph_4Sb]^+$ is tetrahedral. The geometrical characteristics of O,O′-chelating ligands are typical for catecholates [3,24,25]. In general, molecular structure of complex **7** in solid state is close to earlier reported structures of complexes $[Ph_4Sb]^+[(beetle\text{-}Cat)_2SbPh_2]^-$ [16] and $[Ph_4Sb]^+[(PhenCat)SbPh_2]^-$ [3a].

3.3. The electrochemical properties

The electrochemical behaviour of complexes was studied by means of cyclic voltammetry in dichloromethane solutions using glass carbon working electrode, Ag/AgCl/KCl(sat.) reference

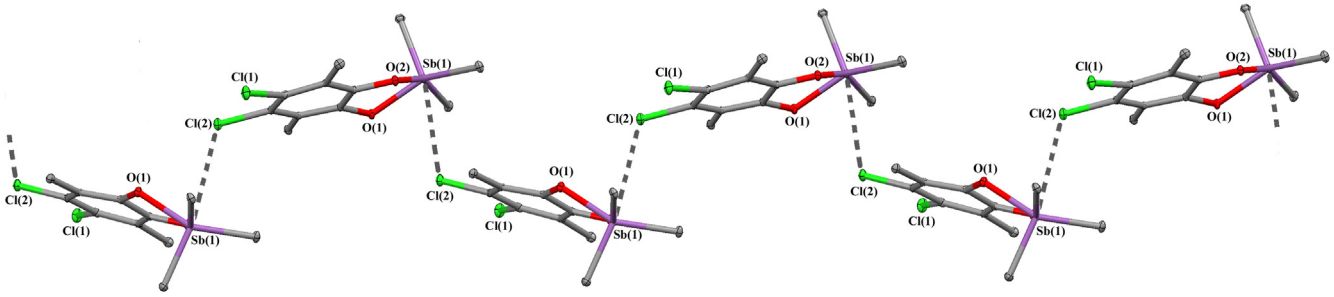

Fig. 2. The intermolecular Sb(1) … Cl (2) interactions in 1D coordination polymeric chain (methyl groups of tert-butyls, phenyls, hydrogen atoms are not shown for clarity).

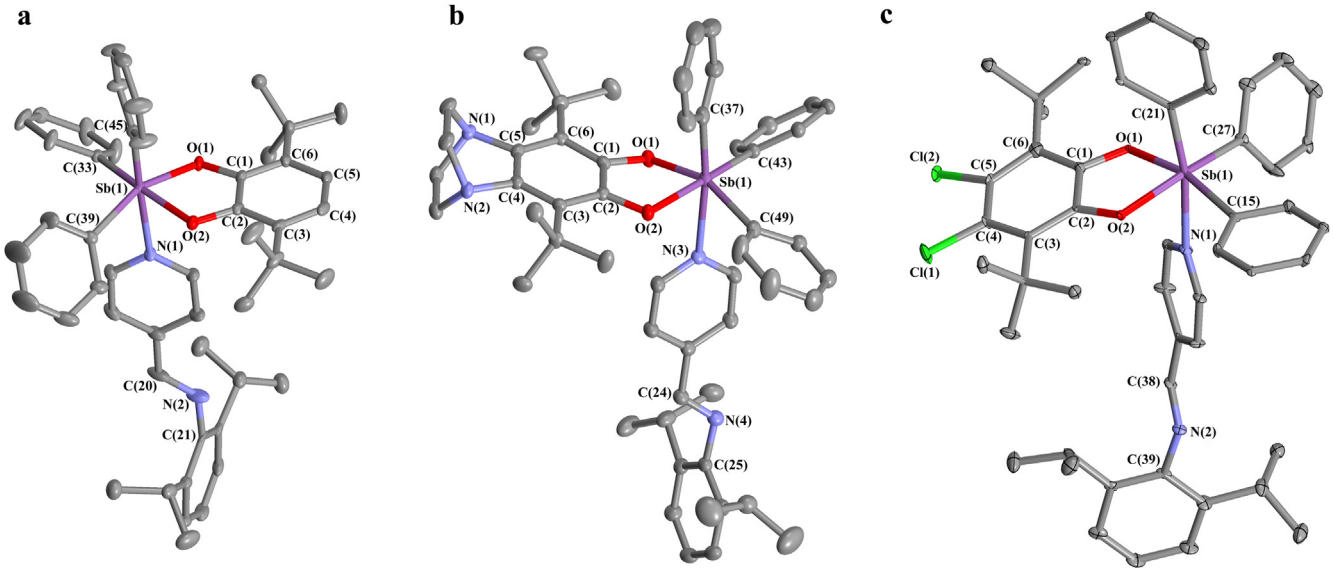

Fig. 3. The molecular structures of complexes **4** (a), **5** (b) and **6** (c) in crystals of **4**, **5**·1.6n-hexane and **6**, respectively. The ellipsoids are given with 50% probability. The hydrogen atoms are omitted for clarity.

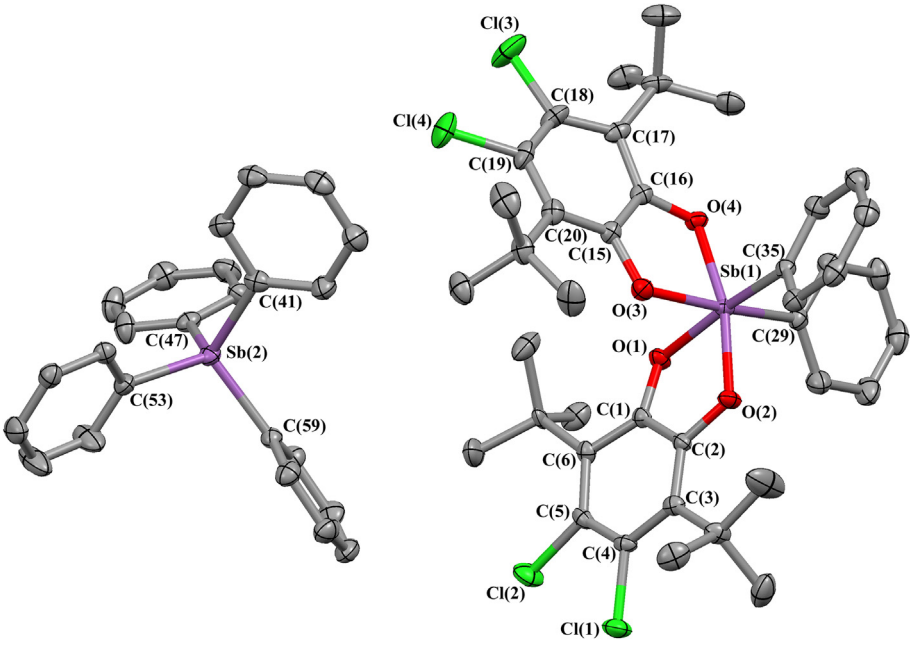

Fig. 4. The molecular structure of **7** in crystals (ellipsoids of 50% probability). The hydrogen atoms are omitted.

Table 4
The CV data for triphenylantimony(V) catecholates (CH_2Cl_2, GC anode, $C = 3 \cdot 10^{-3}$ M, in argon, 0.15 M Bu_4NClO_4, vs Ag/AgCl/KCl).

N	Compound	$E^{ox1}{}_p$[b], V	n	$E^{ox2}{}_p$[b], V
1	(3,6-DBCat)$SbPh_3$	0.96 (0.89)	1	1.40
2[c]	(4,5-pip-3,6-DBCat)$SbPh_3$[a]	0.76	1	1.23 (1.15)
3	(4,5-Cl_2-3,6-DBCat)$SbPh_3$	1.03 (0.97)	1	1.33
4	(3,6-DBCat)$SbPh_3$·(Py-CH=N–Ar)	0.94	2	1.83
5[c]	(4,5-pip-3,6-DBCat)$SbPh_3$·(Py-CH=N–Ar)	0.74	1	1.15 (1.09)
6	(4,5-Cl_2-3,6-DBCat)$SbPh_3$·(Py-CH=N–Ar)	0.99	2	1.84
8	(3,6-DBCat)$SbPh_3$·Py	0.93	2	–

[a] The data from Ref. [17].
[b] The values of $E^{ox}{}_{1/2}$ for quasi-reversible processes are given in brackets.
[c] $E^{ox3}{}_p = 1.48$ V.

electrode. The electrochemical data are given in Table 4.

The oxidation of initial triphenylantimony(V) catecholate **1** proceeds as two successive one-electron oxidations (Scheme 3): the first one, $E^{ox1}{}_{1/2} = 0.89$ V, is the reversible oxidation wave Cat/SQ, the second one, $E^{ox2}{}_p = 1.40$ V, is irreversible wave SQ/Q [5b,11a]. The electrochemical oxidation of chloride-substituted complex **3** has the same electrochemical profile as in the case of compound **1** (Scheme 3, Fig. S15). The modification of catecholate ring of the redox-active ligand in the fourth and fifth positions by the electron withdrawing chlorine atoms decreases the stability of the *o*-semiquinonato form 4,5-Cl_2-3,6-DBBQ of redox-active ligand ($I_c/I_a = 0.65$) formed during the oxidation as compared with previously studied complex **1** (for **1**, the current ratio $I_c/I_a = 0.82$ [5b,26]). The first oxidation peak for complex **3** is shifted to the anodic area (0.07 V) in the accordance with electron withdrawing effect of chlorine atoms.

The electrochemical behaviour of triphenylantimony(V) catecholate **8** containing a coordinated pyridine molecule differs from that one for **1** (Fig. S13): one two-electron peak is observed instead of two anodic peaks. The general mechanism of the oxidation includes one irreversible two-electron stage (at $E^{ox}{}_p = 0.93$ V) insignificantly shifted to the cathode region as compared with $E^{ox1}{}_p$ for **1**. A controlled-potential microelectrolysis of **8** was performed at 1.1 V that corresponds to the potential value at which the catecholate ligand is oxidized. The data of coulometric measurements have established that pyridine adduct **8** is double-electron-oxidized yielding a dicationic derivative $\mathbf{8}^{2+}$ (Scheme 3).

The same situation takes place in the case of iminopyridine-containing complexes **4** and **6**. In the range of potentials from −0.6–1.4 V the oxidation of these compounds also proceeds as one two-electron irreversible stage at 0.94 and 0.99 V (Fig. 5(1,3)). The first oxidation process leads to the formation of dicationic species $\mathbf{4}^{2+}$ (Scheme 4) and $\mathbf{6}^{2+}$ containing doubly oxidized form of redox-active ligand. The coulometric measurements performed at the potential 1.1 V have confirmed that complexes **4** and **6** undergo two-electron-oxidation at this stage. In case of the targeted compounds, the small variation of electrochemical

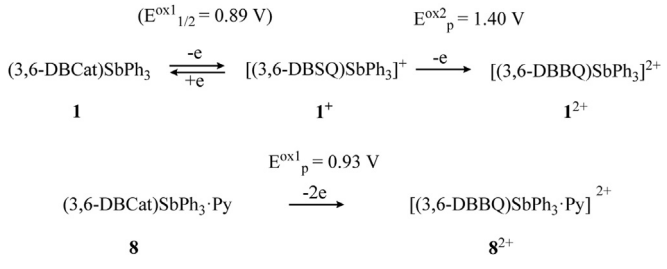

Scheme 3. The electrochemical oxidation of complexes **1** and **8**.

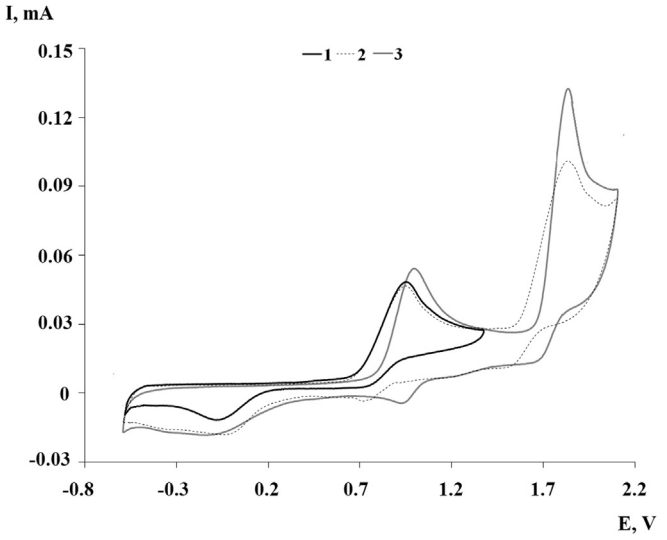

Fig. 5. The CVs of (3,6-DBCat)$SbPh_3$·(Py-CH=N–Ar) (**4**) (curve 1 – the potential range from −0.60–1.40 V; curve 2 – the potential range from −0.60–2.1 V) and (4,5-Cl_2-3,6-DBCat)$SbPh_3$·(Py-CH=N–Ar) (**6**) (curve 3 – the potential range from −0.60 to 2.1 V). (CH_2Cl_2, GC electrode, $C = 3 \times 10^{-3}$ M, 0.1 M NBu_4ClO_4, $V = 0.2$ V s^{-1}, vs. Ag/AgCl/KCl(sat.)).

potentials ($E^{ox1}{}_p$) suggests a partial transfer of electron density from the iminopyridine ligand to the central antimony atom.

The irreversibility of the first anodic stages in both cases (**4** and **6**) implies the subsequent chemical stage in the solution - the decoordination of *o*-benzoquinone ligand from the dicationic intermediates $\mathbf{4}^{2+}$ and $\mathbf{6}^{2+}$. This is confirmed by the impulse potential sweep: in the range from −0.7–1.4 V in the pulse potential scanning mode, it possible to observe the quasi-reversible redox transition at the value of potential −0.53 V corresponding to the reduction of decoordinated o-benzoquinone (Fig. S14). The expansion of potential range to 2.1 V (Fig. 5(2)) allows to observe another anodic peak at the high anodic value of potential (1.83 V). This oxidation step corresponds to the oxidation of iminopyridine ligand in species $[Ph_3Sb\cdot(Py\text{-}CH{=}N{-}Ar)]^{2+}$. Free iminopyridine Py-CH=N–Ar undergoes the electrochemical oxidation at $E^{ox}{}_p = 1.66$ V [27]. Thus, the general scheme of redox-processes for complexes **4** and **6** may be presented as it is shown on the example of complex **4** (Scheme 4):

In contrast to catecholate **4** and **6**, the electrochemical behaviour of piperazine-containing catecholate **5** (Scheme 4) does not practically differ from that one for initial catecholate **2** [16]. The oxidation mechanism in case of **5** does not change (Scheme 5).

The coordination of iminopyridine ligand to **2** with a formation of **5** does not leads to the remarkable redistribution of electron density. It may be connected with the influence of piperazine moiety, and the initial participation of piperazine moiety in the oxidation and intramolecular electron transfer between two redox-active fragments of ligand (Scheme 5). The values of peak potentials of the first and the second anodic processes shift slightly to the cathode region due to the increase of the electron density caused by a coordinated pyridine-containing ligand Py-CH=N–Ar. The third anode stage at 1.48 V for **5** (as well as **2**) corresponds to the deeper oxidation of redox-active ligand.

Also the fourths oxidation stage was observed at the high anodic potential at 1.85 V. As well as in the case of **4** or **6**, the wave at 1.85 V is the oxidation of iminopyridine ligand in species $[Ph_3Sb\cdot(Py\text{-}CH{=}N{-}Ar)]^{2+}$.

It should be noted that piperazine-containing catecholate **5** despite the pyridine coordination on the antimony atom has the

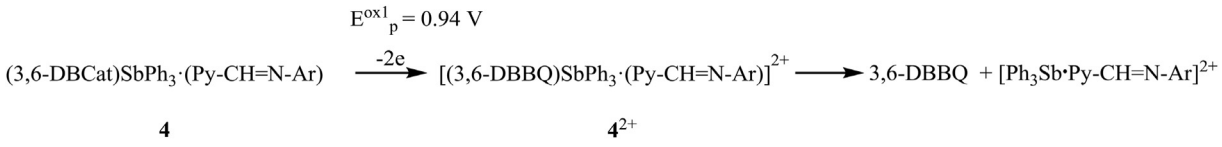

Scheme 4. The electrochemical oxidation of **4**.

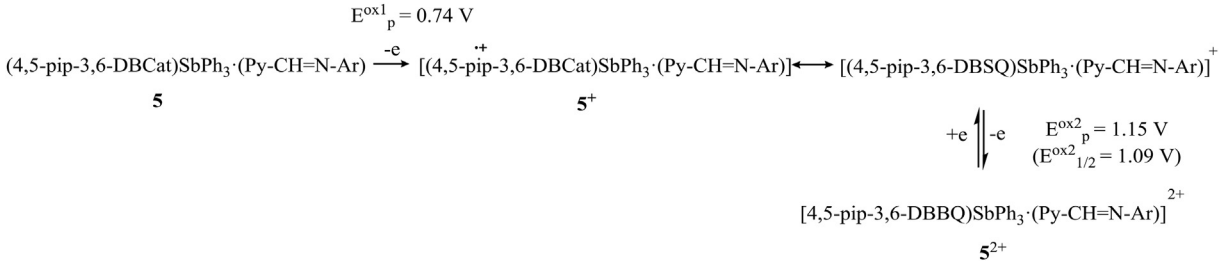

Scheme 5. The electrochemical oxidation of **5**.

tendency to interact with air oxygen. The fixation of CV in the presence of oxygen leads to the changes in CV curve (Fig. 6): the shift of the oxidation peaks to the cathode region, the decrease of their current intensity, and the appearance of the additional redox-stage at +1.34 V corresponding to the oxidation of spiroendoperoxide [16]. The analogical changes take place in the reaction of triphenylantimony(V) 4,5-dimethoxy-3,6-di-*tert*-butyl-catecholate with bromide anion under aerobic conditions. This complex as compound **4** is able to bind molecular oxygen. Aeration of solution promotes bromide anion elimination from the antimony coordination sphere with the formation of spiroendoperoxide compound [28].

4. Conclusions

Triphenylantimony(V) catecholates (3,6-DBCat)$SbPh_3$ (**1**), (4,5-pip-3,6-DBCat)$SbPh_3$ (**2**) and (4,5-Cl_2-3,6-DBCat)$SbPh_3$ (**3**) readily react with 4-(2,6-dimethylphenyliminomethyl)pyridine (Py-CH═N–Ar) or pyridine to form new hexacoordinate complexes (3,6-DBCat)$SbPh_3$·(Py-CH═N–Ar) (**4**), (4,5-pip-3,6-DBCat)$SbPh_3$·(Py-CH═N–Ar) (**5**), (4,5-Cl_2-3,6-DBCat)$SbPh_3$·(Py-CH═N–Ar) (**6**) and (3,6-DBCat)$SbPh_3$·Py (**8**) where the central antimony atom is additionally coordinated by Py-CH═N–Ar or Py as a neutral donor ligand. In the absence of donor ligands chlorine-containing catecholate **3** undergoes rearrangement in acetonitrile to form ionic complex $[Ph_4Sb]^+[(4,5\text{-}Cl_2\text{-}3,6\text{-}DBCat)_2SbPh_2]^-$ (**7**). Complexes have been isolated and characterized by spectroscopic methods and cyclic voltammetry.

The molecular structures of complexes **3**–**7** in crystals have been determined by single-crystal X-ray analysis. In crystal of **3**, complex molecules form 1D polymeric structure due to the additional intermolecular interactions between chlorine atoms in Cat ligand and the central antimony atoms. Complexes **4**–**6** possess a distorted octahedral geometry with the equatorial plane formed by oxygen atoms of the chelating redox-active catecholato ligand and atoms with two phenyl substituents, while $N_{Pyridine}$-coordinated iminopyridine is disposed on the apical site. The cyclic voltammetry studies have shown the different effect of a iminopyridine coordination on the electrochemical behaviour of complexes. Complexes undergo a series of. The presence of $N_{Pyridine}$-coordinated iminopyridine ligand changes the mechanism of catecholate oxidation in **4** and **6** (as compared with **1** and **3**): the first oxidation wave is two-electron and corresponds to the oxidation of dianionic catecholate ligand to a coordinated *o*-benzoquinone (the initial complexes **1** and **3** undergo two successive one-electron oxidation stages leading to monocationic *o*-semiquinonato and dicationic quinonato derivatives, respectively). In contrast to catecholates **4** and **6**, the electrochemical behaviour of piperazine-containing catecholate **5** does not practically differ from that one for initial catecholate **2**.

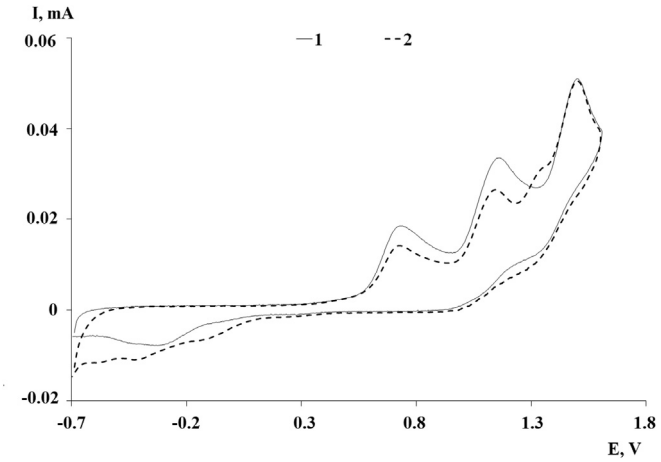

Fig. 6. The CVs of compound (4,5-pip-3,6-DBCat)$SbPh_3$·(Py-CH═N–Ar) (**5**) (curve 1 – under argon conditions; curve 2 – after 20 min under aerobic conditions) at the potential range from −0.70 to 1.6 V (CH_2Cl_2, GC electrode, $C = 1 \times 10^{-3}$ M, 0.1 M NBu_4ClO_4, V = 0.2 V s^{-1}, vs. Ag/AgCl/KCl(sat.)).

Acknowledgements

The work was performed in the framework of the Russian state assignment. The physic-chemical investigations were performed using the instrumental base of the Analytical Center of the G.A. Razuvaev Institute of Organometallic Chemistry, Russian Academy of Sciences.

Appendix A. Supplementary data

Supplementary data to this article can be found online at https://doi.org/10.1016/j.jorganchem.2019.06.025.

References

[1] a) Y. Matano, Chapter 9.10, antimony and bismuth, in: P. Knochel (Ed.), Comprehensive Organometallic Chemistry III vol. 9, Elsevier, 2007, pp. 425–456. Applications I: Main Group Compounds in Organic Synthesis;
b) N. Farrell, Chapter 9.18. Metal complexes as drugs and chemotherapeutic agents, in: M.D. Ward (Ed.), Comprehensive Coordination Chemistry II, vol. 9, Elsevier, Amsterdam, 2005, pp. 809–840;
c) R. Ge, H. Sun, Acc. Chem. Res. 40 (2007) 267–274;
d) A.M. Christianson, F.P. Gabbaï, Antimony- and bismuth-based materials and applications, in: T. Baumgartner, F. Jackle (Eds.), Main Group Strategies towards Functional Hybrid Materials, Wiley, 2018, pp. 405–432.

[2] a) W. Levason, G. Reid, Chapter 3.6. Arsenic, antimony, and bismuth, in: J.A. McCleverty, T.J. Meyer (Eds.), Comprehensive Coordination Chemistry II, vol. 3, Elsevier, Amsterdam, 2005, pp. 465–544;
b) H.J. Breunig, R. Wagner, Chapter 3.16. Arsenic, antimony, and bismuth organometallics, in: C.E. Housecroft (Ed.), Comprehensive Organometallic Chemistry III, vol. 3, Elsevier, Amsterdam-Boston-Heidelberg, 2007, pp. 905–930;
c) A.I. Poddel'sky, Chapter 12. Antimony complexes with o-quinonato ligands and related O,N-, O,N,O-, O,N,O,O-ligands, in: M. Razeghi (Ed.), Antimony: Characteristics, Compounds and Applications, Nova Science Publishers, New York, 2012, pp. 267–302;
d) V.A. Kuropatov, S.V. Klementieva, A.I. Poddel'sky, V.K. Cherkasov, G.A. Abakumov, Russ. Chem. Bull., Int. Ed. 59 (2010) 1698–1706;
e) Ch-H. Chen, F.P. Gabbai, Angew. Chem. Int. Ed. 56 (2017) 1799–1804;
f) M. Yang, N. Pati, G. Bélanger-Chabot, M. Hiraia, F.P. Gabbaï, Dalton Trans. 47 (2018) 11843–11850;
g) D. You, H. Yang, S. Sen, F.P. Gabbaï, J. Am. Chem. Soc. 140 (2018) 9644–9651;
h) C.H. Chen, F.P. Gabbaï, Dalton Trans. 47 (2018) 12075–12078;
i) Y.-H. Lo, F.P. Gabbaï, Organometallics 37 (2018) 2500–2506.

[3] a) V.K. Cherkasov, G.A. Abakumov, E.V. Grunova, A.I. Poddel'sky, G.K. Fukin, E.V. Baranov, YuA. Kurskii, L.G. Abakumova, Chem. Eur J. 12 (2006) 3916–3927;
b) G.K. Fukin, I.A. Guzei, E.V. Baranov, G.A. Domrachev, Struct. Chem. 20 (2009) 643–654;
c) D. Tofan, F.P. Gabbai, Chem. Sci. 7 (2016) 6768–6778;
d) I.-Sh Ke, J.S. Jones, F.P. Gabbai, Angew. Chem. Int. Ed. 53 (2014) 2633–2637.

[4] a) Sh Ye, B. Sarkar, F. Lissner, Th Schleid, J. Slageren, J. Fiedler, W. Kaim, Angew. Chem. Int. Ed. 44 (2005) 2103–2106;
b) A.V. Piskunov, A.V. Maleeva, G.K. Fukin, V.K. Cherkasov, A.S. Bogomyakov, Inorg. Chim. Acta 455 (2017) 213–220;
c) V.I. Ovcharenko, E.V. Gorelik, S.V. Fokin, G.V. Romanenko, V.N. Ikorskii, A.V. Krashilina, V.K. Cherkasov, G.A. Abakumov, J. Am. Chem. Soc. 129 (2007) 10512–10521.

[5] a) N.A. Protasenko, A.I. Poddel'skii, I.V. Smolyaninov, N.T. Berberova, G.K. Fukin, V.K. Cherkasov, G.A. Abakumov, Russ. Chem. Bull., Int. Ed. 63 (2014) 930–937;
b) A.I. Poddel'sky, I.V. Smolyaninov, YuA. Kurskii, N.T. Berberova, V.K. Cherkasov, G.A. Abakumov, Russ. Chem. Bull., Int. Ed. 58 (2009) 532–537.

[6] a) R. Hernandez Molina, A. Mederos, 1.19. Acyclic and macrocyclic schiff base ligands, in: A.B.P. Lever (Ed.), Comprehensive Coordination Chemistry II, vol. 1, Elsevier-Pergamon Press, Amsterdam - Oxford - New York, 2003, pp. 411–446;
b) F. Villafañe, Coord. Chem. Rev. 339 (2017) 128–137;
c) M. Zahedi, B. Shaabani, M. Aygün, C. Kazak, Inorg. Chim. Acta 469 (2018) 461–468;
d) M. Zahedi, B. Shaabani, U. Englert, N. Rad-Yousefnia, G.R. Blake, C. Kazak, Polyhedron 133 (2017) 110–118.

[7] a) A.A. Trifonov, Eur. J. Inorg. Chem. (2007) 3151–3167;
b) H.P. Nayek, N. Arleth, I. Trapp, M. Löble, P. Oña-Burgos, M. Kuzdrowska, Y. Lan, A.K. Powell, F. Breher, P.W. Roesky, Chem. Eur J. 17 (2011) 10814–10819;
c) K. Kowolik, M. Shanmugam, T.W. Myers, C.D. Cates, L.A. Berben, Dalton Trans. 41 (2012) 7969–7976;
d) A.A. Trifonov, T.V. Mahrova, L. Luconi, G. Giambastiani, D.M. Lyubov, A.V. Cherkasov, L. Sorace, E. Louyriac, L. Maron, K.A. Lyssenko, Dalton Trans. 47 (2018) 1566–1576.

[8] a) A.A. Tehrani, A. Morsali, M. Kubicki, Dalton Trans. 44 (2015) 5703–5712;
b) M. Khanpour, A. Naghipour, A.A. Tehrani, A. Morsali, D. Morales-Morales, S. Hernandez-Ortega, J. Mol. Struct. 1135 (2017) 26–31;
c) A.A. Kissel, D.M. Lyubov, T.V. Mahrova, G.K. Fukin, A.V. Cherkasov, T.A. Glukhova, D. Cuib, A.A. Trifonov, Dalton Trans. 42 (2013) 9211–9225;
d) A. Ch Kalita, S.K. Gupta, R. Murugavel, Chem. Eur J. 22 (2016) 6863–6875.

[9] a) M.Y. Masoomi, S. Beheshti, A. Morsali, J. Mater. Chem. 2 (2014) 16863–16866;
b) G.K. Patra, P.K. Pal, J. Mondal, A. Ghorai, A. Mukherjee, R. Saha, H.-K. Fun, Inorg. Chim. Acta 447 (2016) 77–86;
c) N. Rad-Yousefnia, B. Shaabani, M. Kubicki, M.S. Zakerhamidi, A.M. Grzeskiewicz, Polyhedron 129 (2017) 38–45;
d) H. Ghasempour, A.A. Tehrani, A. Morsali, J. Wang, P.C. Junk, CrystEngComm 18 (2016) 2463–2468.

[10] a) I.V. Smolyaninov, N.A. Antonova, A.I. Poddel'sky, S.A. Smolyaninova, V.P. Osipova, N.T. Berberova, J. Organomet. Chem. 696 (2011) 2611–2620;
b) I.V. Smolyaninov, A.I. Poddel'skii, N.A. Antonova, S.A. Smolyaninova, N.T. Berberova, Russ. J. Coord. Chem. 39 (2013) 165–174;
c) I.V. Smolyaninov, A.I. Poddel'sky, E.O. Korchagina, S.A. Smolyaninova, N.T. Berberova, Dokl. Phys. Chem. 460 (2015) 45–48.

[11] a) I.V. Smolyaninov, A.I. Poddel'skiy, N.T. Berberova, V.K. Cherkasov, G.A. Abakumov, Russ. J. Coord. Chem. 36 (2010) 644–650;
b) A.I. Poddel'sky, YuA. Kurskii, A.V. Piskunov, N.V. Somov, V.K. Cherkasov, G.A. Abakumov, Appl. Organomet. Chem. 25 (2011) 180–189;
c) G.K. Fukin, E.V. Baranov, A.I. Poddel'sky, V.K. Cherkasov, G.A. Abakumov, ChemPhysChem 13 (2012) 3773–3776;
d) S.A. Chesnokov, N.A. Lenshina, M.V. Arsenyev, R.S. Kovylin, M.A. Baten'kin, A.I. Poddel'sky, G.A. Abakumov, Appl. Organomet. Chem. 31 (2017), e3553.

[12] a) I.V. Smolyaninov, N.A. Antonova, A.I. Poddel'sky, V.P. Osipova, M.N. Kolyada, N.T. Berberova, Dokl. Chem. 443 (2012) 72–76;
b) I.V. Smolyaninov, N.A. Antonova, A.I. Poddel'sky, V.P. Osipova, N.T. Berberova, YuT. Pimenov, Appl. Organomet. Chem. 26 (2012) 277–283;
c) I.V. Smolyaninov, N.A. Antonova, A.I. Poddel'sky, S.A. Smolyaninova, V.P. Osipova, S.A. Luzhnova, N.T. Berberova, YuT. Pimenov, Appl. Organomet. Chem. 28 (2014) 274–279;
d) I.V. Smolyaninov, A.I. Poddel'skii, S.A. Smolyaninova, N.O. Movchan, Russ. J. Gen. Chem. 84 (2014) 1761–1766.

[13] W.L. F Armarego, D.D. Perrin, in: Purification of Laboratory Chemicals, fourth ed., Butterworth-Heinemann, Oxford, 1996.

[14] V.K. Cherkasov, E.V. Grunova, A.I. Poddel'sky, G.K. Fukin, YuA. Kurskii, L.G. Abakumova, G.A. Abakumov, J. Organomet. Chem. 690 (2005) 1273–1281.

[15] G.A. Abakumov, V.K. Cherkasov, T.N. Kocherova, N.O. Druzhkov, YuA. Kurskii, M.P. Bubnov, G.K. Fukin, L.G. Abakumova, Russ. Chem. Bull. 56 (2007) 1849–1856.

[16] A.I. Poddel'sky, I.V. Smolyaninov, YuA. Kurskii, G.K. Fukin, N.T. Berberova, V.K. Cherkasov, G.A. Abakumov, J. Organomet. Chem. 695 (2010) 1215–1224.

[17] H.-H. Perkampus, B. Behjati, J. Heterocycl. Chem. 11 (1974) 511–514.

[18] G.M. Sheldrick, SHELXTL V. 6.14, Structure Determination Software Suite, Bruker AXS, Madison, Wisconsin, USA, 2003.

[19] CrysAlis Pro - Software Package, Agilent Technologies, 2012.

[20] Bruker, SADABS, Bruker AXS, Madison, Wisconsin, USA, 2014.

[21] A.I. Poddel'sky, I.V. Smolyaninov, N.V. Somov, N.T. Berberova, V.K. Cherkasov, G.A. Abakumov, J. Organomet. Chem. 695 (2010) 530–536.

[22] D.R. Lide (Ed.), CRC Handbook of Chemistry and Physics, CRC Press, Boca Raton, FL, 2005.

[23] S.S. Batsanov, Russ. J. Inorg. Chem. 36 (1991) 3015–3037.

[24] a) A.M. Christianson, E. Rivard, F.P. Gabbai, Organometallics 36 (2017) 2670–2676;
b) A.I. Poddel'sky, E.V. Baranov, G.K. Fukin, V.K. Cherkasov, G.A. Abakumov, J. Organomet. Chem. 733 (2013) 44–48;
c) M. Hirai, F.P. Gabbai, Chem. Sci. 5 (2014) 1886–1893;
d) A.I. Poddel'sky, I.V. Smolyaninov, N.T. Berberova, G.K. Fukin, V.K. Cherkasov, G.A. Abakumov, J. Organomet. Chem. 789–790 (2015) 8–13;
e) M. Hirai, F.P. Gabbai, Angew. Chem. Int. Ed. 54 (2015) 1205–1209;
f) A.I. Poddel'sky, I.V. Smolyaninov, G.K. Fukin, N.T. Berberova, V.K. Cherkasov, G.A. Abakumov, J. Organomet. Chem. 824 (2016) 1–6;
g) A.I. Poddel'sky, N.O. Druzhkov, G.K. Fukin, V.K. Cherkasov, G.A. Abakumov, Polyhedron 124 (2017) 41–50.

[25] a) A.M. Christianson, E. Rivard, F.P. Gabbai, Organometallics 36 (2017) 2670–2676;
b) A.I. Poddel'sky, M.V. Arsenyev, T.V. Astaf'eva, S.A. Chesnokov, G.K. Fukin, G.A. Abakumov, J. Organomet. Chem. 835 (2017) 17–24;
c) M.V. Arsenyev, T.V. Astaf'eva, E.V. Baranov, A.I. Poddel'sky, S.A. Chesnokov, Mendeleev Commun. 28 (2018) 76–78;
d) A.I. Poddel'sky, I.V. Smolyaninov, G.K. Fukin, N.T. Berberova, V.K. Cherkasov, G.A. Abakumov, J. Organomet. Chem. 867 (2018) 238–245;
e) M.V. Arsen'ev, L.S. Okhlopkova, A.I. Poddel'skii, G.K. Fukin, Russ. J. Coord. Chem. 44 (2018) 162–168;
f) A.I. Poddel'sky, T.V. Astaf'eva, I.V. Smolyaninov, M.V. Arsenyev, G.K. Fukin, N.T. Berberova, V.K. Cherkasov, G.A. Abakumov, J. Organomet. Chem. 873 (2018) 57–65.

[26] A.I. Poddel'sky, I.V. Smolyaninov, Russ. J. Gen. Chem. 80 (2010) 538–540.

[27] Data in CH_2Cl_2, GC Anode, $C = 3 \cdot 10^{-3}$ M, in Argon, 0.15 M Bu_4NClO_4, vs Ag/AgCl/KCl(sat.).

[28] A.I. Poddel'skii, E.V. Ilyakina, I.V. Smolyaninov, G.K. Fukin, N.T. Berberova, V.K. Cherkasov, G.A. Abakumov, Russ. Chem. Bull. 63 (2014) 923–929.